17th Australasian Fluid Mechanics Conference
Auckland, New Zealand
5-9 December 2010

On Modelling Horizontal Gas-Liquid Flow using Population Balance Approach

C. Li[1], G.H. Yeoh[2,3], S.C.P. Cheung[1] and J.Y. Tu[1]
[1] School of Aerospace, Mechanical and Manufacturing Engineering,
RMIT University, Victoria 3083, Australia
[2] School of Mechanical and Manufacturing Engineering,
University of New South Wales, Sydney 2052, Australia
[3] Australian Nuclear Science and Technology Organisation (ANSTO)
Locked Bag 2001 Kirrawee DC, NSW 2232, Australia

Abstract

In this study, the performance of population balance model based on Average Bubble Number Density approach has been assessed to predict internal phase distributions of gas-liquid bubbly flow in a horizontal pipe. Predicted local radial distributions of void fraction, interfacial area concentration and gas velocity have been validated against the experimental data [3] under four flow conditions with average gas volume fraction ranging from 4.4% to 20%. Generally speaking, the predicted results have achieved satisfactory agreements with measured values. Some discrepancies have nonetheless been found between the numerical and experimental results at certain locations of the pipe. The insufficient resolution of the turbulent model in fully accommodating the strong turbulence in the current pipe orientation and the inclusion of additional interfacial force such as the prevalent bouncing force among bubbles remain some of the outstanding challenging issues need to be addressed in order to improve the prediction of horizontal gas-liquid bubbly flow.

Introduction

In industrial application, various equipments and facilities have been commonly running under horizontal bubbly gas-liquid flow conditions since it has capability to provide large interfacial areas for mass and heat transfer in general and in particular for the attachment of particles. A typical example of industrial application is bitumen extraction process, which requires three major procession stages, namely liberation of bitumen from the sand grains; attachment of the liberated bitumen with air bubbles; and flotation of bitumen-air aggregates to form a bitumen-rich froth. It is evident that the bubble diameter or interfacial area concentration (interfacial surface area per unit volume) plays a significant role on the efficiency of the attachment and flotation in bitumen extraction process. According to Sanders et al. [1], bitumen droplets have shown the tendency of attaching to the air bubbles of similar sizes. Furthermore, air injection can reduce energy assumption by helping bitumen recovery at lower process temperature (<50^{o}C). Since the size distribution of injected air bubbles can significantly influence bitumen processing system, the development of suitable modeling and simulation techniques capable of determining the size distribution in horizontal bubbly flow is indeed vital for the design and safe operation of bitumen hydro-transport system.

In retrospective, most concern of two-phase gas-liquid flows have been focused on vertical configurations while horizontal gas-liquid flows have received considerably less attention in the literature. In vertical flows, buoyant force acts towards either the same as (upward flow) or the opposite to (downward flow) flow main direction. It balances with the drag force and mainly affects the gas-liquid relative velocity at the axial direction, but does not induce any lateral asymmetry in either the velocity or phase distribution. In horizontal flows, the buoyant force is nonetheless in the direction perpendicular to the flow main direction. It imposes an additional strong radial force, which causes a significant flow asymmetry. Thereby, under the combination of radial and axial forces, bubbles can travel neither vertically nor horizontally, which increases the difficulty in modeling horizontal gas-liquid flow in comparison to vertical gas-liquid flow.

Several measurement techniques have been utilized to describe the internal structure of horizontal bubbly flows. Kocamustafaogullari et al. [2, 3] described an experimental study on local interfacial parameters in a horizontal bubbly two-phase flow. Andreussi [4] proposed a new We_{cr} correlation to identify the transition between dispersed bubble flow and elongated bubble flow. Recently, interfacial structure of horizontal bubbly flow has been observed in 45-degree and 90-degree elbow by Kim et al. [5, 6]. For numerical studies, the semi-empirical drift flux model has been developed to predict the integral flow characteristics of horizontal bubbly flows by Haoues et al [7] and Talley and Kim [8]. Teslishcheva et al [9] applied the two-fluid model to simulate the void fraction and velocity profiles in a long straight horizontal pipe and a similar pipe with a 90-degree elbow. However, all the numerical researches mentioned above were studied under assumption of constant bubble diameter without consideration of bubble realistic interaction mechanisms. In gas-liquid flows, the local spatial two-phase geometrical internal structure (bubble diameter or interfacial area concentration) is affected by the coalescence and break-up through the interactions among bubbles as well as between bubbles and turbulent eddies in turbulent flows. In order to aptly predict the particle size distribution, the population balance equation can be applied to handle the complicated bubble interaction mechanisms. Ekambara et al [10] have applied the MUltiple Size Group (MUSIG) model to investigate internal phase distribution of horizontal bubbly flow. In the MUSIG model, the continuous particle size distribution is discretized into series number of discrete size classes; the mass conservation of each size fractions are balanced by source terms which represent inter-fraction mass transfer due to the mechanisms of bubble coalescence and breakage processes. Computationally, as the number of transport equations depends on the number of group adopted, the MUSIG model generally requires large computational time and resources to achieve stable and accurate numerical predictions.

In the present of work, a simpler population balance model based on the Average Bubble Number Density approach is assessed in

simulating the internal phase distributions of air-water bubbly flow in an inner diameter of 50.3mm horizontal pipeline. Four flow conditions with average gas volume fraction from 4.4% to 20% were investigated. The predicted local radial distributions of void fraction, Interfacial Area Concentration (IAC) and gas velocity are compared against the experimental data of Kocamustafaogullari and Huang [3].

Mathematical Models

Two-Fluid Model

Two-fluid model treats the general case of modelling each phase or component as a separate fluid with its own set of governing balance equations and bridging these separate phase through appropriate constitutive relations governing the inter-phase mass, momentum and energy exchanges. For isothermal bubbly flow without the heat and mass transfer, the three-dimensional two-fluid model conservation equations comprise the mass and momentum conservation equations. They are:

$$\frac{\partial(\rho_i \alpha_i)}{\partial t} + \nabla \cdot (\rho_i \alpha_i \vec{u}_i) = 0 \qquad (1)$$

$$\frac{\partial(\rho_i \alpha_i \vec{u}_i)}{\partial t} + \nabla \cdot (\rho_i \alpha_i \vec{u}_i \vec{u}_i) = -\alpha_i \nabla P_i + \alpha_i \rho_i \vec{g} + F_i + \nabla \cdot \left[\alpha_i \mu_i^e \left(\nabla \vec{u}_i + (\nabla \vec{u}_i)^T \right) \right] \qquad (2)$$

The subscript i can be f or g, representing liquid or gas phase, respectively. Relevant constitutive relationships for the interfacial forces, suitable turbulent model and population balance model are required to achieve closure of the two-fluid model equations, which are described below.

Interfacial Forces

In equation (2), F_i represents the total interfacial forces calculated with averaged variables, which consist of the momentum exchanges between the liquid and bubble phases in two-fluid model. Appropriate consideration of different sub-forces affecting the interaction between each phase can be formulated for isothermal bubbly flow as:

$$F_i = F_i^{\text{drag}} + F_i^{\text{lift}} + F_i^{\text{lubrication}} + F_i^{\text{dispersion}} \qquad (3)$$

The sub-forces appearing on the right hand side of equation (3) are: drag, lift, wall lubrication and turbulent dispersion. The interfacial drag force is a result of the shear and form drag of the fluid flow which depends on the drag coefficient as well as the interfacial area concentration. The Ishii and Zuber [11] drag coefficients under consideration of different flow regimes are employed for current research. Due to radial velocity gradient, bubbles in a liquid are subjected to a radial lift force. For the lift coefficient, Tomiyama [12] correlations have been considered. In contrast to the lift force, wall lubrication force constitutes another radial force due to surface tension allowing bubble concentrated in a region close to the wall, but not immediately adjacent to the wall. This results in a low void fraction at the vicinity of the wall area. In this study, wall lubrication force model proposed by Antal et al. [13] has been employed. By considering turbulent assisted bubble dispersion, turbulence dispersion force has been exerted as a function of turbulent kinetic energy in the continuous phase and gradient of the volume fraction according to Antal et al. [13]

Turbulence Modelling

The Menter's [14] Shear Stress Transport (SST) model that accounts for the transport of the turbulent shear stress for the liquid phase is employed in the present study. The SST model is a hybrid version of $k-\varepsilon$ and $k-\omega$ models with a specific blending function. It allows resolution of the flow explicitly down to the wall boundary instead of the use of empirical wall function to bridge the wall and the far-away turbulent flow.

Population Balance Model

In order to represent bubble interaction mechanisms caused by the effects of coalescence and break-up through the interactions among bubbles as well as between bubbles and turbulent eddy in turbulent flows, the population balance model has been applied. In current study, an Average Bubble Number Density model recently proposed by Yeoh and Tu [15] has been applied. The averaged bubble number density can be expressed as:

$$\frac{\partial n}{\partial t} + \nabla \cdot (\vec{u}_g n) = \phi_n^{RC} + \phi_n^{TI} + \phi_n^{WE} \qquad (4)$$

where $n = 6\alpha_g / \pi D_s^3$ is the average bubble number density. The phenomenological mechanisms of coalescence and breakage are affected through the source and sink terms: ϕ_n^{RC}, ϕ_n^{TI} and ϕ_n^{WE} of which they are due to random collision, turbulent induced breakage and wake entrainment. The Yao and Morel [16] model is adopted in the present study, *viz.*,

$$\phi_n^{RC} = -C_{RC1} \frac{(\alpha_g)^2 (\varepsilon_l)^{1/3}}{D_s^{11/3}} \frac{\exp\left(-C_{RC2}\sqrt{We/We_{cr}}\right)}{\left(\alpha_{max}^{1/3} - \alpha^d\right)/\alpha_{max}^{1/3} + C_{RC3}\alpha^d \sqrt{We/We_{cr}}} \qquad (5)$$

$$\phi_n^{TI} = C_{TI1} \frac{\alpha_g (1-\alpha_g)(\varepsilon_l)^{1/3}}{D_s^{11/3}} \frac{\exp(-We_{cr}/We)}{1 + C_{TI2}(1-\alpha_g)\sqrt{We/We_{cr}}} \qquad (6)$$

where $C_{RC1} = 2.86$, $C_{RC2} = 1.017$, $C_{RC3} = 1.922$, $C_{TI1} = 1.6$ and $C_{TI2} = 0.42$. The critical Weber number We_{cr} of 1.42 is suggested by Yao and Morel [16]. Considering the transition point from the finely dispersed bubbly flow to slug flow, the maximum allowable void fraction α_{max} retains a value of 0.52. According to Hibiki and Ishii [17], wake entrainment phenomenon only plays significant influence in slug flow. In this study, wake entrainment has been ignored.

Numerical Details

The 3-D numerical model of air-water bubbly flow in an inner diameter of 50.3mm horizontal pipeline is assessed against the experiments conducted by Kocamustafaogullari and Huang [3]. An O-grid is generated for the cross-sectional plane of the long horizontal pipe such as illustrated in Figure 1. Table 1 summarizes the inlet boundary conditions for the various bubbly flows under consideration. At the inlet of the test section, uniformly distributed superficial liquid and gas velocities and

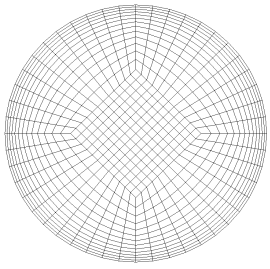

Figure 1: cross-sectional plane of the computational mesh for bubbly flow investigation in a long horizontal pipe

void fraction are assumed in accordance with the flow conditions.

The uniform injected bubble diameter of 3 mm is assumed according to the experimental data [3] at the location of z/D = 25, where the bubble diameter is similar to the one at inlet. The validation between the numerical results and experimental values have been performed at $\theta = 0°$ over the cross-section at the location of z/D = 253. The angle θ is calculated from top.

Table 1. Bubbly flow conditions and its inlet boundary conditions employed in the present study

Superficial liquid velocity $\langle j_f \rangle$ *(m/s)*	*Superficial gas velocity* $\langle j_g \rangle$ *(m/s)*	
	0.213 m/s	**0.419 m/s**
4.670 m/s	[4.4]	[8.5]
$[\alpha_g\|_{z/D=0.0}$ (%)]	[3.0]	[3.0]
	0.788 m/s	**1.210 m/s**
$[D_S\|_{z/D=0.0}$ (mm)]	[14.6]	[20.46]
	[3.0]	[3.0]

Results and Discussion

Time Averaged Gas Void Fraction

The predicted radial void fraction distribution of horizontal bubbly flow comparing against experimental data of Kocamustafaogullari and Huang [3] at the dimensionless axial position z/D = 253 are shown in Figure 2. It can be seen from the gas void fraction profiles that a peak persisted in the vicinity of the upper wall of the pipe, which was caused by the buoyant force being migrated upward gas bubbles balancing with a wall lubrication force being exerted downward. In contrast to vertical bubbly flow, the movement of bubble towards the wall is, in general, caused by the balance between the lift and wall lubrication forces. It can also be seen from the experiments that with the increasing of interfacial gas velocities from $\langle j_g \rangle$ = 0.213 m/s to $\langle j_g \rangle$ = 0.788 m/s the peak value of gas void fraction increased up to 0.6, which has exceeded the maximum allowable void fraction of 0.52. It indicated that gas bubbles have reached the saturation limit at the upper wall. Further increasing the superficial gas velocity to $\langle j_g \rangle$ = 1.210 m/s did not show any appreciable increase of the peak gas void fraction in the vicinity of the upper wall. Rather, the local gas void fraction began to increase at the lower half of the pipe indicating the likelihood of gas bubbles migrating downwards.Generally, the model predictions of the local gas void fraction are in good agreement with all the experimental conditions except for the superficial gas velocity $\langle j_g \rangle$ = 1.210 m/s. At this superficial gas velocity, the model underestimated the local gas void fraction at the lower half of the pipe. One possible explanation could be the insufficiency of the turbulence-induced force to dramatically push the bubbles away from the top pipe wall or the requirement to add a wall reaction force such as prevalent bouncing force to counterbalance the buoyant force within horizontal bubbly flow. Nevertheless, the wall reaction force remains to be fully tested and deserves separate thorough investigation in the future.

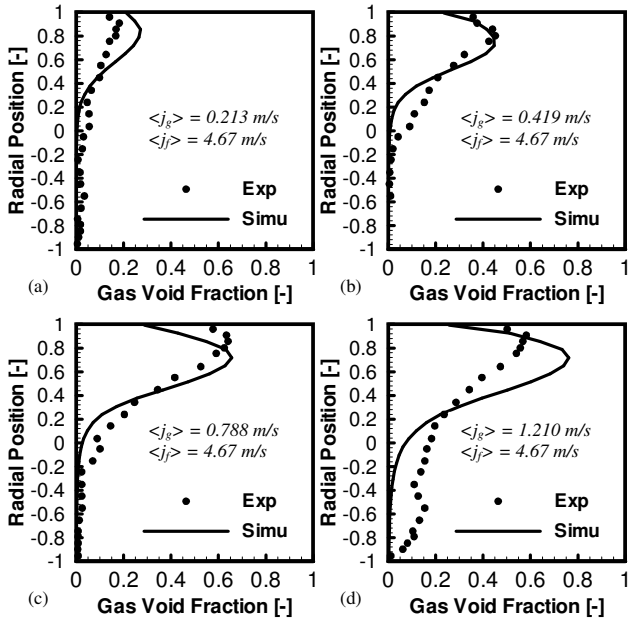

Figure 2: Predicted radial void fraction distributions and experimental data of Kocamustafaogullari and Huang [3] at location of L/D = 253

Time Averaged Interfacial Area Concentration (IAC)

Figure 3 illustrates the predicted and measure Interfacial Area Concentration (IAC) corresponding to the void fraction profile in Figure 2. With the assumption of spherically-shaped bubbles, the IAC can be simply calculated by local void fraction α_g and Sauter mean diameter D_s through:

$$a_{if} = \frac{6\alpha_g}{D_s} \tag{7}$$

As shown in Figure 3, the model yielded reasonable prediction comparing with experimental data except for the underestimation of IAC peak at the vicinity of the wall for the interfacial gas velocities of $\langle j_g \rangle$ = 0.419 m/s and $\langle j_g \rangle$ = 0.788 m/s. This was probably due to the lack of robustness of the model constants adopted in the Yao and Morel [16] model which required calibration in order to aptly predict the bubble size within the isothermal bubbly flow for these conditions.

Time Averaged Gas Velocity

Figure 4 shows the comparison of predicted and experimental

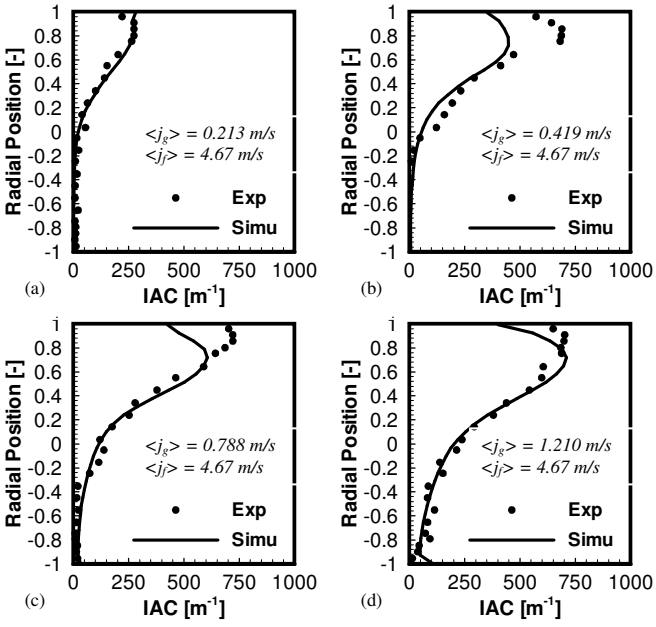

Figure 3: Predicted Interfacial Area Concentration (IAC) distributions and experimental data of Kocamustafaogullari and Huang [3] at location of L/D = 253

data of axial components of gas velocity profiles. The experimental data demonstrated that changes in the velocity profile shape are very small compared with the changes in the void fraction and IAC. There are no peaks in gas velocity profile corresponding to those observed toward the top wall peaking in void fraction and IAC. Similar phenomena have also been observed in vertical bubbly flow. In vertical bubbly flow condition, bubble accelerates along axial direction driving by the strong buoyant force, gas bubbles therefore rises faster than liquid while liquid velocities in gas-liquid flow system are greater than ones in single phase flow system under the same flow conditions due to the inertial force between gas and liquid. However, in horizontal bubbly flow condition, the buoyant force which is perpendicular to flow axial direction has a lesser contribution in pushing the gas bubble to move along axial direction than that in vertical bubbly flow. According to Kocamustafaogullari and Huang [3] liquid velocities are slightly greater than the bubble velocities and the bubbles are accelerated by liquid inertia in a very short distance after injection and the local gas phase velocities follow closely the local liquid phase velocities. As seen in Figure 3, the numerical results are in reasonable prediction with the experimental data.

Conclusions

In this study, the internal phase distributions of air-water bubbly flow in an inner diameter of 50.3 mm horizontal pipeline have been investigated using the two-fluid and ABND models. The predicted local radial distributions of void fraction, IAC and gas velocity have been validated against the experimental data of Kocamustafaogullari and Huang [3].

In general, satisfactory agreements between predicted and measured results were achieved. The results indicated that the local gas void fraction and IAC peaked near the upper pipe wall because of the strong buoyant effect. The gas velocity profiles corresponded to fully-developed turbulent pipe-flow profiles, which meant highly non-symmetric void fraction has less influence on the gas velocity distribution. Some discrepancies were found between the numerical and experimental results. Better turbulent model to capture the physical processes associated with complex turbulent bubbly flow in horizontal pipe or additional interfacial force such as bouncing force among bubbles may need to be considered to further improve the model predictions.

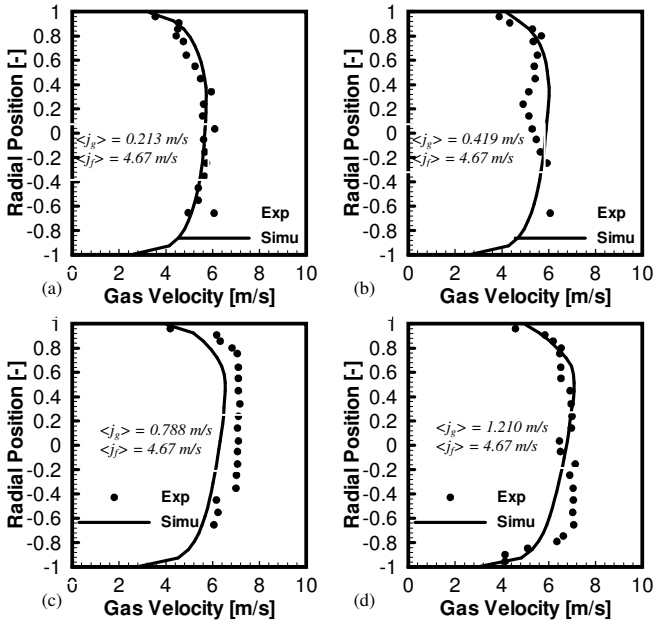

Figure 4.Precicted gas velocity distributions and experimental data of Kocamustafaogullari and Huang [3] at location of L/D = 253

References

[1] Sanders, R. S., Razzaque, M. M., Schaan, J., Nandakumar, K., Masliyah, J. H., Afacan, A., Shijie, L. Bubble size distributions for dispersed air - Water flows in a 100 mm horizontal pipeline. *Can. J. Chem. Eng.*, **82,** 2004, 858-864.

[2] Kocamustafaogullari, G., Wang, Z. "An experimental study on local interfacial parameters in a horizontal bubbly 2-phase flow. *Int. J. Multiphase Flow*, **17**, 1991, 553-572.

[3] Kocamustafaogullari, G. Huang, W. D. "Internal structure and interfacial velocity development for bubbly 2-phase flow. *Nucl. Eng. Des.*, ***151***, 1994, 79-101.

[4] Andreussi, P., A. Paglianti, et al. Dispersed bubble flow in horizontal pipes. *Chem. Eng. Sci.*, **54**, 1999, 1101-1107.

[5] Kim, S., Park, J. H., Kojaosy, G., Kelly, J. M., Marshall, S. O. Geometric effects of 90-degree Elbow in the development of interfacial structures in horizontal bubbly flow. *Nuc. Eng. Des.*, **237,** 2007, 2105-2113.

[6] Kim, S., Callender, K., Kojasoy, G. Interfacial area transport in horizontal bubbly flow with 90-degree elbow. *Nuc. Tech.*, **167**, 2009, 20-28.

[7] Haoues, L., Olekhnovitch, A., Teyssedou, A. Numerical study of the influence of the internal structure of a horizontal bubbly flow on the average void fraction. *Nuc. Eng. Des.*, **239**, 2009, 147-157.

[8] Talley, J. D., Kim, S. Horizontal bubbly flow with elbow restrictions: Interfacial area transport modeling. *Nuc. Eng. Des.* **240**, 2010, 1111-1120.

[9] Tselishcheva, E. A., Antal, S. P., Podowski, M. "Mechanistic multidimensional analysis of horizontal two-phase flows. *Nuc. Engi. Des.*, **240**, 2010, 405-415.

[10] Ekambara, K., Sanders, R. S., Nandakumar, K., Masliyah, J. H. CFD simulation of bubbly two-phase flow in horizontal pipes. *Chem. Eng. J.*, **144**, 2008). 277-288.

[11] Ishii, M., Zuber, N. "Drag coefficient and relative velocity in bubby, droplet or particulate flows. *AIChE J.*, **25**, 1979, 843-855.

[12] Tomiyama, A. (2004). Drag, lift and virtual mass forces acting on a single bubble. *3rd International Symposium on Two-phase Flow Modelling and Experimentation*, Pisa, 22-24.

[13] Antal, S. P., R. T. Lahey, et al. Analysis of phase distribution in fully-developed laminar bubbly 2-phase flow. *Int. J. Multiphase Flow*, **17**, 1991, 635-652.

[14] Menter, F. R. 2-equation eddy-viscosity turbulence models for engineering applications. *AIAA J.*, **32**, 1994, 1598-1605.

[15] Yeoh, G. H., Tu, J. Y. Numerical modelling of bubbly flows with and without heat and mass transfer. *Appl. Math. Model.*, **30**, 2006, 1067-1095.

[16] Yao, W., Morel, C. Volumetric interfacial area prediction in upward bubbly two-phase flow. *Int. J. Heat Mass Transfer*, **47**, 2004, 307-328.

[17] Hibiki T., Ishii M., Development of one-group interfacial area transport equation in bubbly flow systems, Int. J. Heat Mass Trans. **45**, 2002, 2351–2372.